TITLE: Detection of early osteogenic commitment in primary cells using Raman spectroscopy

AUTHORS: Stephanie J. Smith, Roger Emery, Andrew Pitsillides, Claire E. Clarkin and Sumeet Mahajan

JOURNAL TITLE: Analyst

PUBLICATION DATE: May 2017

PUBLISHER: Royal Society of Chemistry

DOI: 10.1039/C6AN02469F

Detection of early osteogenic commitment in primary cells using Raman spectroscopy

Stephanie J. Smith[1], Roger Emery[2], Andrew Pitsillides[3], Claire E. Clarkin[1†*], Sumeet Mahajan[4†*].

[1]Department of Biological Sciences, University of Southampton, SO17 1BJ, U.K.
[2]Division of Surgery, Reproductive Biology and Anaesthetics, Imperial College London, U.K
[3]Department of Veterinary Basic Science, Royal Veterinary College, London, NW1 0TU, U.K.
[4]Department of Chemistry and the Institute for Life Sciences, University of Southampton SO17 1BJ, U.K.

*Correspondence to: s.mahajan@soton.ac.uk, c.e.clarkin@soton.ac.uk
† Authors contributed equally to this study

Abstract

Major challenges in the development of novel implant surfaces for artificial joints include osteoblast heterogeneity and the lack of a simple and sensitive *in vitro* assay to measure early osteogenic responses. Raman spectroscopy is a label-free, non-invasive and non-destructive vibrational fingerprinting optical technique that is increasingly being applied to detect biochemical changes in cells. In this study Raman spectroscopy has been used to obtain bone cell-specific spectral signatures and to identify any changes therein during osteoblast commitment and differentiation of primary cells in culture. Murine calvarial osteoblasts (COBs) were extracted and cultured and studied by Raman spectroscopy over a 14 day culture period. Distinct osteogenic Raman spectra were identified after 3 days of culture with strong bands detected for mineral: phosphate υ_3 (1030 cm^{-1}) and B-type carbonate (1072 cm^{-1}), DNA (782 cm^{-1}) and collagen matrix (CH_2 deformation at 1450 cm^{-1}) and weaker phosphate bands (948 and 970 cm^{-1}). Early changes were detected by Raman spectroscopy compared to a standard enzymatic alkaline phosphatase (ALP) assay and gene expression analyses over this period. Proliferation of COBs was confirmed by fluorescence intensity measurements using the Picogreen dsDNA reagent. Changes in ALP levels were evident only after 14 days of culture and mRNA expression levels for ALP, Col1a1 and Sclerostin remained constant during the culture period. Sirius red staining for collagen deposition also revealed little change until day 14. In contrast Raman spectroscopy revealed the presence of amorphous calcium phosphate (945-952 cm^{-1}) and carbonated apatite (957-962 cm^{-1}) after only 3 days in culture and octacalcium phosphate (970 cm^{-1}) considered a transient mineral phase, was detected after 5 days of COBs culture. PCA analysis confirmed clear separation between time-points. This study highlights the potential of Raman spectroscopy to be utilised for the early and specific detection of proliferation and differentiation changes in primary cultures of bone cells.

1. Introduction

Studies of bone forming osteoblast cells have significant medical impact with stimulation of osteoblast formation and activation continuing to have wide clinical demand. Although bone exhibits some highly conserved factors in its development, remodelling and repair, it is also apparent that the response to many *in vivo* challenges is not always consistent in different regions of bone [1-3]. These observations suggest that osteoblast populations are inherently heterogeneous and support a current hypothesis that their identity is specific to their local environment [4]. In recent attempts to clinically improve the success of joint replacement much focus has been on the study of the bone cell-implant interface with the long term success of joint replacement relying on sufficient osteoblast adherence, proliferation and differentiation in promoting osseointegration in specific regions. [5-7]. Historically, successful osseointegration has been assessed post implantation radiographically. However the study of osteoblast activity *in vitro* on implant surfaces could improve the development of implant coatings and allow for more accurate predictions of posteoperative osseointegration success. While in this paper we study osteoblast activity on quartz cover slips it is relevant and will provide insight for implant surfaces, subsequent studies and their modelling.

Osteoblast cells derive from mesenchymal progenitors and transition to pre-osteoblasts before finally becoming bone forming osteoblasts [8]. The differentiation process of osteoblasts is often defined by the presence of these three different-stage cell types but their identities are not yet clearly defined. Early transgenic studies describe the genes required for osteoblast differentiation [9, 10]. It is now generally accepted that transcription factors Runx2, osterix and β-catenin are involved in the regulation of osteoblast differentiation [11]. Currently, identifying mesenchymal progenitor commitment to the osteoblast lineage is in the expression of Runx2 and osterix, at which point they are considered pre-osteoblasts [12, 13]. Mature osteoblasts are characterised by their ability to secrete large amounts of extracellular proteins including osteocalcin alkaline phosphatase (ALP) and type I collagen, the main constituents of osteoid matrix which forms prior to osteoblast commitment and

mineralisation [8, 14]. The final stage of bone formation is mineralisation which is thought to initiate with the formation of hydroxyapatite (HA) crystals inside matrix vesicles (MVs) which are 50-200 nm in diameter and bud from the surface membrane of hypertrophic chondrocytes and osteoblasts [15-18]. Inorganic calcium (Ca^{2+}) and phosphate (Pi) ions accumulate inside MVs instigating the breakdown of the MV membrane, releasing HA crystals into the extracellular fluid where they propagate on the collagenous extracellular matrix [16, 19-21]. Inorganic phosphate ions also play a key role in regulating mineralisation.

During *in vitro* bone formation, expression of mature osteoblast specific genes and subsequent mineralisation typically takes place between 14 to 28 days [22, 23]. An ability to detect and quantify osteoblast differentiation early during the culture process is attractive in the comparative study of distinct osteoblast populations and also clinically for evaluating growth on implant surfaces. Raman spectroscopy, an optical vibrational finger-printing technique, is label-free, non-invasive and non-destructive and can be a more sensitive means compared to conventional biochemical methods to detect osteogenesis.

Raman spectroscopy has gained a lot of interest in recent years as a potential diagnostic tool for detecting such early biochemical changes in cells [24]. Raman spectroscopy has also indeed been widely applied to characterise bone and its constituents [25-27]. Its capability to detect bone nodule formation in *in vitro* secondary cell cultures has also been demonstrated although under high mineralisation conditions [28, 29]. Recently the application of Raman spectroscopy to grade live osteosarcoma cells was also investigated by Chiang *et al*, who measured levels of hydroxyapatite produced by osteosarcoma cell lines, a possible measure of malignancy [30]. By characterising the Raman signatures of different cell types, researchers have been able to apply this technique to monitor the differentiation of stem cells with Raman effectively monitoring the osteogenic differentiation of human mesenchymal stem cells (hMSCS) from 7 days of *in vitro* culture [31]. Hung *et al* also used hMSCs to investigate matrix formation as a measure of maturation of live hMSCs [32]. Although this paper has demonstrated the feasibility of using Raman

spectroscopy to quantitatively analyse hMSC maturity, here we perform a thorough investigation on primary osteoblast cells isolated directly from murine neonatal bone tissue, and have been able to detect and characterise spectral changes over 14 days of culture due to proliferation, differentiation and deposition of matrix in osteoblasts. Whilst Hung *et al* were unable to detect early amorphous forms of calcium phosphate, we were able to not only detect different transient mineral species, but also quantify changes over time. Moreover, we study osteoblast cultures in natural growth (physiological) rather than over-mineralising conditions most often used by Raman researchers studying similar bone cells or osteogenesis [29]. Furthermore, we show that these changes are observed by Raman spectroscopy earlier than typical enzymatic and gene expression assays. Our study therefore establishes Raman spectroscopy as a simple, label-free, non-invasive and non-destructive alternative tool for assessing primary bone cultures and early changes therein with many applications in the field of skeletal regeneration.

2. Materials and Methods

2.1 Reagents

All tissue culture reagents, including α Minimum essential medium (αMEM) (no. 22571) and fetal calf serum (FCS) (no. 102701) were purchased from Invitrogen Life Technologies (Paisley, UK). All other reagents were purchased from Sigma unless otherwise stated.

2.2 Isolation and culture of calvarial osteoblasts.

Primary mouse calvarial osteoblasts (COBs) were obtained by sequential enzyme digestion of excised calvarial bone from 4-day-old neonatal mice (c57/bl6) using a 4-step process (CCEC; [50]). The first digest (1 mg/ml collagenase type Ⅱ in HBSS for 10 min) was discarded. The following 3 digests (fraction 1, 1 mg/ml collagenase type Ⅱ in HBSS for 30 min; fraction 2, 4 mM EDTA in PBS for 10 min; fraction 3, 1 mg/ml collagenase type Ⅱ in HBSS for

30 min) were retained. During the final digestion, the cells obtained from fractions 1 and 2 were resuspended in αMEM supplemented with 10% heat-inactivated FCS (HI FCS), 5% gentamicin, 100 U/ml penicillin, 100 µg/ml streptomycin. The cells from fraction 3 were then combined with fractions 1 and 2 for expansion. The cells were cultured in 75 cm^2 flasks (6 calvaria/ flask) for 7 days in a humidified atmosphere of 5% CO_2-95% air at 37˚C until confluent.

Upon confluence COBs were either plated into 12 well tissue culture plates or quartz coverslips (UQG optics CFQ-1017 #No1.5, thickness: 0.17 mm, Ø 10) at density of 7900 cells/cm^2. Cells were cultured for 3, 5, 7 and 14 days in αMEM supplemented with osteogenic media containing 50µg/ml ascorbic acid (AA) and 2.5 mM β- Glycerophosphate (BGP). For Raman spectroscopy COBs were fixed with 4% w/v paraformaldehyde and stored in PBS prior to imaging.

2.3 Alkaline Phosphatase activity elution assay and staining

COBs for elution assay were grown in 12 well plates as described above, washed twice with PBS before treating with 100% ethanol for 1 minute. Fixative was removed and cells were washed twice in distilled water. P-nitrophenol substrate (1mg/ml) was then added to a working solution of 70% dH20, 20% 0.1M NaHCO3 and 10% 30mM $MgCl_2$, pH was adjusted to 9.5. 500 µl of working solution was added to each well and incubated for 30 minutes at 37°C. 2x200 µl of eluted solution was removed and pipetted into a 96 well plate. Absorbance was measured after 1 minute at 405 nm. Concentration of nmols/ml/minute was calculated using a standard curve of known concentrations of p-nitrophenol solution (0.05, 0.1, 0.15, 0.2, 0.25mM).

ALP activity was also visualised by histochemical staining at day 3, and 14. After fixation with methanol: acetone cells were rinsed then treated with naphthol AS-MX as a substrate and Fast blue to produce a coloured precipitate.

2.4 Sirius Red collagen staining

To visualise collagen deposition over time, Sirius red staining was performed at days 3, 5, 7 and 14. COBs were grown in 12 well plates at a density of 5 x 10^4 cells/well, with and without BGP and AA. After the desired culture period, cells were washed twice with PBS before fixing with 70% ethanol for 1 hour. After fixation, cells were dried at 37°C and stained with Sircol Dye Reagent (Biocolor, County Antrim, UK) for 1 hour. After staining, cells were washed with dH_20 and allowed to air dry.

2.5 RNA Extraction and cDNA synthesis

After removal of culture media and washing with PBS, COBs were disrupted with lysis buffer. Lysates were stored at -80°C before RNA extraction. Total RNA was isolated using Qiagen RNeasy Mini Kit according to the manufacturer's instructions. The RNA for each sample was determined using a Nanodrop UV-vis spectrophotometer. cDNA was synthesised using the RT2 First Strand Kit (Qiagen catalogue #330401). Osteogenesis array carried out using PAMM-026ZA-6 - RT² Profiler™ Mouse Osteogenesis PCR Array (Qiagen catalogue #33023). Used Bio-Rad/MJ Research Chromo4 thermal cycler. Thermal cycling conditions included a 10 minute HotStart DNA Taq activation step at 95°C, followed by 40 cycles of 95°C for 15 seconds and 55°C for 30 seconds. A melting curve was included with temperature increase from 65°C to 95°C with 0.2°C increments for 1 second.

2.6 Genomic DNA isolation and Picogreen assay

COBs for genomic DNA extraction were cultured in 6 well plates as described above. After desired culture period, medium was removed and cells were washed with PBS, before the addition of 250 µl Trypsin/EDTA. An equal volume of α- MEM medium was added to the cells after dissociation to neutralise the trypsin. COBs were transferred to an Eppendorf and centrifuged at 10,000 RPM for 5 minutes. Pelleted cells were resuspended in 200 µl PBS and PureLink™Genomic DNA MiniKit was used to isolate genomic DNA according to manufacturer's instructions.

Once genomic DNA was obtained, the Quant-iT™PicoGreen®dsDNA reagent, a fluoresecent nucleic acid stain was used to quantitate double stranded DNA

present in the genomic DNA isolated from COBs. The fluorescence assay was measured with a Hitachi F2500 fluorescence spectrophotometer. Samples were excited at 480 nm and fluorescence intensity was measured at 520 nm. DNA concentration was determined from a previously generated standard curve of known DNA concentrations (1 µg/ml, 100 ng/ml, 10 ng/ml, 1 ng/ml and a blank of TE buffer only).

2. 7 Raman Spectroscopy

For Raman spectroscopy calvarial osteoblasts (COBs) were cultured for 3, 5, 7 and 14 days in osteogenic media (as previously described) on sterilised quartz coverslips. Cells were washed with Dulbecco's phosphate buffered saline (PBS) before fixing with 4% paraformaldehyde for 5 minutes at room temperature. After fixation COBs were washed in PBS. Raman spectra were obtained using a Renishaw® inVia Raman microscope with a 532 nm laser and a Leica 63x (NA: 1:2) water immersion objective in combination with WIRE 3.4 software. The diffraction limited spot size is ~300 nm. However, we note that the spectral collection was not confocal. Therefore the signal was collected from a focal volume defined by the spot size. For consistency Raman spectra were always collected from single cells over the nucleus. The nucleus was selected as a marker area as it was the most distinctly visible feature of cell in the brightfield image. Spectra were acquired from 20 cells and for each spectrum 2 accumulations of 30 s exposure were collected.

Cosmic ray artefacts were removed using WiRE 3.4. Before plotting the spectra they were processed using IRootLab, a MATLAB based toolbox for vibrational spectroscopy. Prior to general processing, background contribution from quartz was removed. Wavelet denoising and baseline correction was carried out by fitting a 6^{th} order polynomial in IRootlab [33, 34].

2.8 Analysis

Curve fit of Raman peaks carried out using WIRE 3.4 software. Peak heights were measured of class means of the different time points by curve fitting. For evaluating contributions to different biomolecules the fittings were restricted to

the spectral regions of 760-870 cm^{-1} for DNA, 900-980 cm^{-1} for the $\nu_1 PO_4^{3-}$ phosphate region and 1400- 1490 cm^{-1} for the CH_2 deformation (extracellular matrix component of collagen). A number of mixed Gaussian-Lorentzian curves were fitted tor each region. Where possible the curve fitting was initiated by using the same number of peaks although these shifted with the time-course. For example at day 3, 9 peaks were selected to deconvolve the phosphate region, but at day 7 and 14 only 7 were needed. These changes reflect the changes in phosphate disorder [35].

3. Results and Discussion

3.1 Assessment of primary calvarial osteoblasts differentiation by Raman spectroscopy

To assess the differentiation of primary calvarial osteoblasts (COBs) by Raman spectroscopy, osteoblasts were isolated from the calvaria of 4 day old neonate mice by sequential collagenase/EDTA digestion (Figure 1A). Cells were cultured for up to 14 days in standard tissue culture conditions, before fixation with 4% PFA. A single spectrum was collected targeting each cell nucleus. 20 spectra were acquired for a cell culture sample. Overall the COBs' Raman spectra are composed of characteristic biomolecular peaks, first assigned by Puppels, now accepted as biomarkers for cells [36]. Spectra were collected within the "Raman fingerprint region" between 600 cm^{-1} – 1750 cm^{-1}. Strong Raman bands were detected for DNA (782 cm^{-1}) and phenylalanine (1004 cm^{-1}). The quartz cover slip could have contributed to the background (Figure S1) but the strong Raman signal at 782 cm^{-1} is attributable to the cells. The presence of such a large peak in this region has been previously detected in a number of studies [37-39] A range of protein bands associated with collagen and the extracellular matrix were observed including CH_2 deformation at 1450 cm^{-1}, Amide III and Amide I [40]. Mineral bands linked with osteoblasts and bone tissue were also detected namely Phosphate ν_3 (1030 cm^{-1}) and B-type

carbonate (1072 cm^{-1}) as well as weak phosphate bands between 948 and 970 cm^{-1}.

Peak assignment and spectral analysis was carried out on class mean spectra shown in Figure 1C. The class means retain the previously mentioned spectral peaks, highlighted in Figure 1C, and they also display components ascribed to

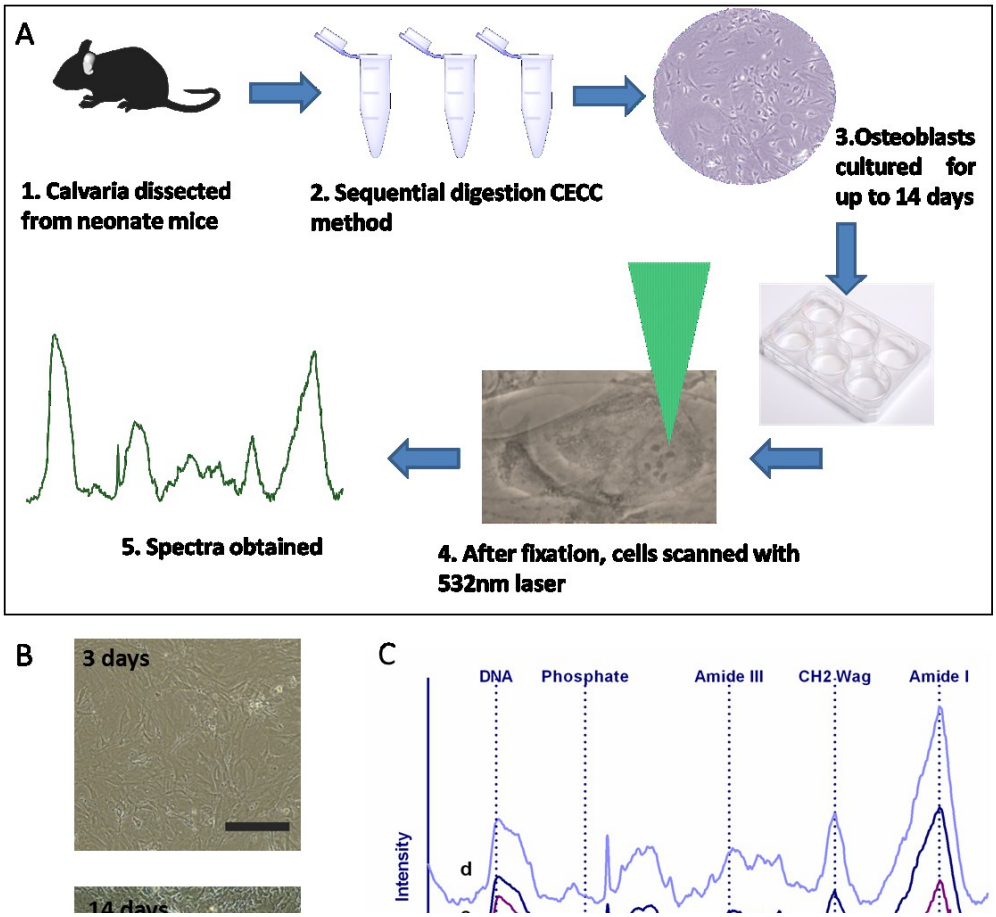

Figure 1. Raman spectroscopy of calvarial osteoblasts (COBs). (A) Schematic of the experimental methodology for this work is shown. Murine calvarial osteoblasts were extracted from 4 day old neonates by sequential collagenase digestion. Cells were cultured up to 14 days on quartz coverslips in standard tissue culture conditions. Following fixation, cell nuclei were scanned with 532 nm laser and spectra obtained from 20 cells per time point. (B) Phase contrast images of COBs in culture highlight phenotypic changes following 14 days of culture in osteogenic media. Scale bar equivalent to 250 µm. (C) Class means of Raman spectra at day 3 (a), 5 (b), 7 (c) and 14 (d). The spectra show differences in key spectral regions over time.

mineralised tissue including Amide I, Amide III, CH_2 deformation for matrix, and Phosphate ν_3 (1030 cm^{-1}) and B-type carbonate (1072 cm^{-1}) bands for mineral [41, 42]. Broad peaks in the phosphate region (948 - 970 cm^{-1}) are also detectable. Before looking at the differences in biochemical composition

provided by Raman spectroscopy, we present the results of biological techniques traditionally used to evaluate osteoblast function.

3.2 **Enzymatic ,mRNA, collagen and DNA measurements of calvarial osteoblasts.**

For assessment of osteoblast maturity and validation of differentiation status, conventional assays and molecular techniques were employed. The Alkaline phosphatase (ALP) activity assay has become the standard assay to measure osteoblast activity *in vitro*. *In vivo*, mature osteoblasts secrete ALP, for which PPi serves as a substrate and when hydrolysed by ALP produces Pi, which accumulates in MVs along with Ca^{2+} during the early phase of mineralisation [21]. *In vitro*, confluent osteogenic cultures are thought to enter an initiation phase after 7 to 14 days, during which time cells will proliferate, express ALP and secrete collagen matrix [43]. The secretion of ALP in osteogenic cultures increases until the cells reach maturation phase and the onset of mineralisation after about 14 – 21 days [23, 43]. Quantitative analysis shows an increase in ALP over time in osteogenic cultures, with the most apparent increase between day 7 and 14 (Fig. 2A).This observation is confirmed by visualisation of ALP activity (Figure 2A; upper panel). Osteoblasts cultured only in basal medium, without the addition of osteogenic mediators (BGP and AA), show little evidence of ALP activity until day 14 of culture. These results highlight that early changes (day 3 to day 7) are not detectable by ALP assay and therefore call for a more sensitive approach.

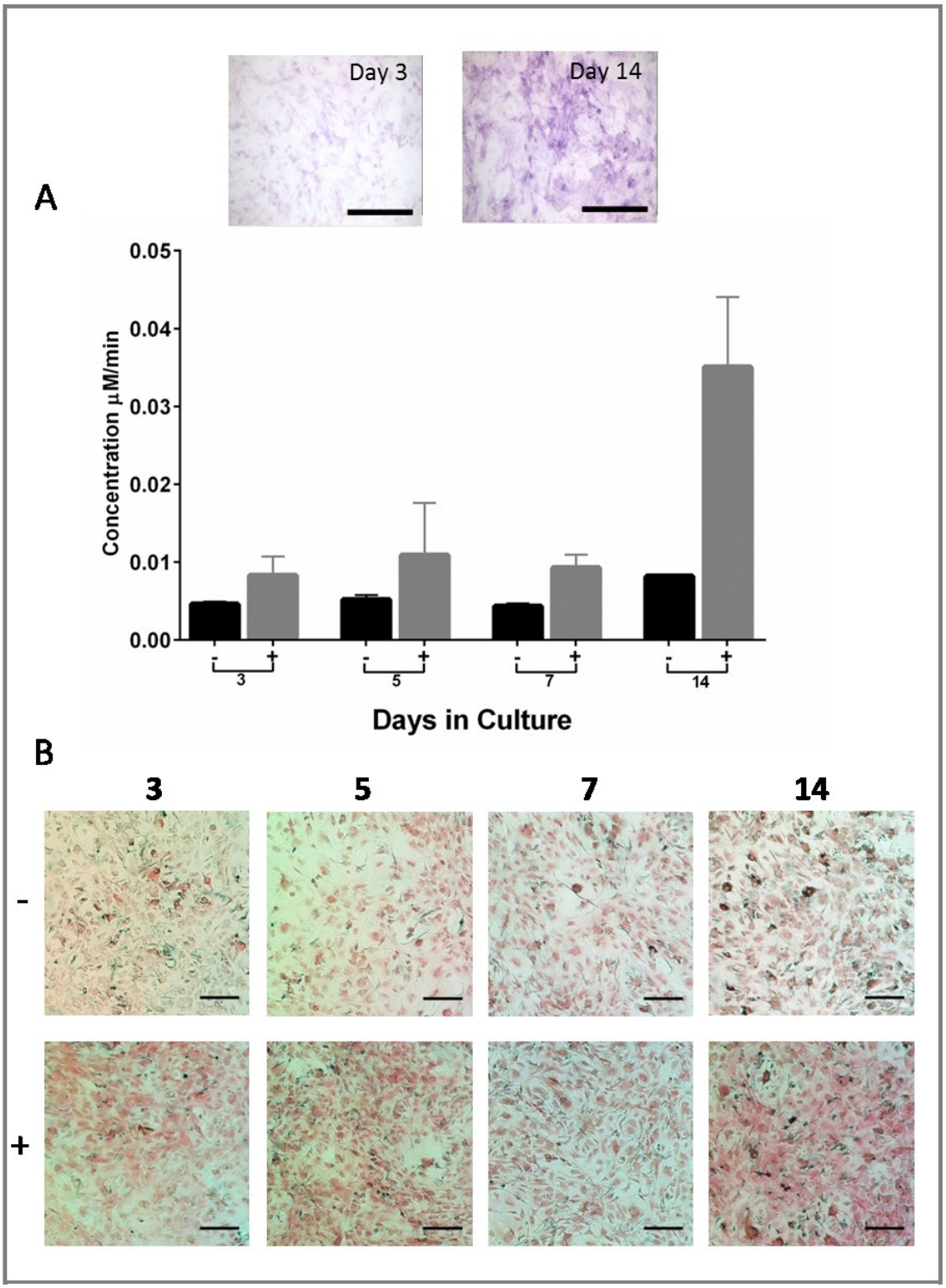

Figure 2. Alkaline Phosphatase (ALP) activity and Sirius red staining of cultured calvarial osteoblasts (COBs). (A) Results for ALP activity are shown. Cells were cultured in osteogenic (+) or basal medium (-), fixed with 100% ethanol and reacted for ALP and eluted. Data are represented as mean concentration of 2 replicates ± STD. The inset shows exemplar images of cells at Day 3 and Day 14 stained for ALP activity. (B) Images for Sirius red staining of COBs for collagen deposition at indicated time points +/- osteogenic media. Scale bar represents 250 µm.

Sirius Red staining for deposited collagen

To assess the deposition of collagen in the COBs cultures over time, cells cultured with and without osteogenic mediators for 3, 5, 7 and 14 days were stained with Sircol Sirius red dye reagent. After staining cells were visualised using phase contrast microscopy (Figure 2B). No obvious differences were detected over time in the cells cultured in non- osteogenic media (Figure 2B, '-' row). COBs that were cultured in osteogenic media (Figure 2B '+' row) reveal a fluctuating increase in collagen deposition over time. Nevertheless, at 14 days the COBs cultured in osteogenic media show the most intense and widespread staining, but little difference is discernible between day 3 and day 5 of osteogenic culture.

mRNA analysis

To confirm COBs were differentiating as expected, RT² Profiler PCR Array Gene Expression Analysis was carried out. From this array a number of genes were selected to investigate osteogenic commitment by COBs; Col1a1 (encodes the major component of collagen type I), SOST (sclerostin, involved in regulation of bone formation in osteoblasts) and ALP (alkaline phosphatase). Interestingly all of these genes show unchanged expression levels between day 5 and day 14 (Figure 3A). This data highlights the lack of sensitivity to effectively detect changes in early *in vitro* osteogenesis. It is not unusual to observe increases in enzymatic activity as seen in the ALP assay between day 7 and day 14 (Figure 2A), that are not mirrored in the mRNA expression. This phenomenon of ALP activity not matching mRNA has been previously reported by Weiss *et al* in a study of the sub-epithelial stroma whereby during gestation ALP activity peaked at day 7, but this elevation in enzyme activity was not preceded by induction of mRNA [44]. Although gene expression analysis can provide some insight into early osteogenic behaviour, it is clear that early detection is not always possible and a more sensitive assay is needed to garner an enhanced understanding of osteogenesis.

DNA quantitation

Early osteogenic commitment is typified by modifications in cellular proliferation. To investigate whether these changes were apparent in our COBs cultures, dsDNA concentration was measured using the Quant-iT™Picogreen® reagent. dsDNA present in genomic DNA isolated from COBs cultured for either 3, 5, 7 or 14 days was quantified by the addition of the Picogreen dye. Samples were

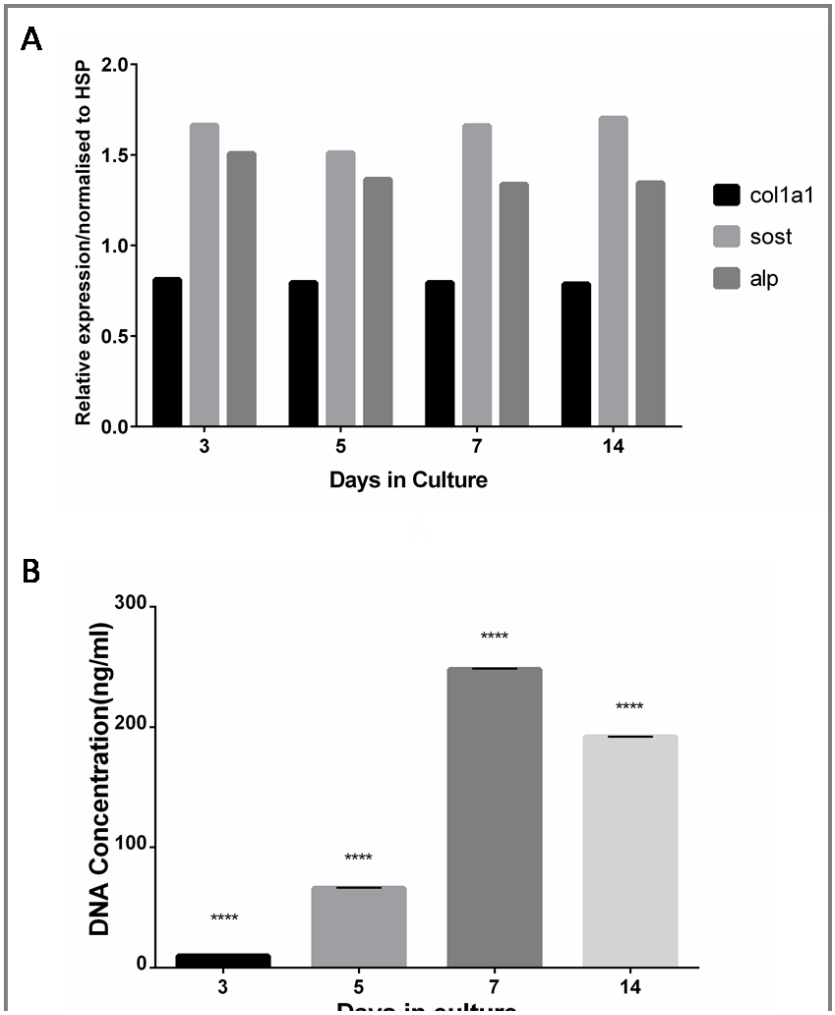

Figure 3. Osteogenic gene expression and fluorescence quantitation of DNA of calvarial osteoblasts cultured for up to 14 days. (A) mRNA expression levels of Col1a1, Sclerostin (SOST) and ALP at different time points. They were normalised to HsP. At each desired time point cells were lysed and RNA was isolated from osteoblasts. After generation of cDNA an RT² Profiler PCR Array was performed comprising one sample per well/gene. (B) Quant-iT™Picogreen® fluorescence intensities of dsDNA isolated from COBs**.** Samples were excited at 480 nm and fluorescence intensity was measured at 520 nm. dsDNA concentration was determined from previously generated standard curve of known DNA concentrations.

excited at 480 nm and fluorescence intensity was measured at 520 nm. Figure 3B shows the concentration of dsDNA present in each time point, determined from a previously generated standard curve of known DNA concentrations. There is an increase in DNA concentration between day 3 and 5 of COBs culture, indicating a proliferation phase. The DNA concentration continues to

increase at day 7. At day 14, however, there is a drop in DNA concentration, suggesting the cells have switched to a proliferative state.

3.3 Raman spectral changes during early osteogenesis identified by univariate deconvolution analysis

To assess whether Raman spectroscopy can indeed allow us to detect early biochemical changes in cells, without losing the heterogeneity of the cell population, in this section, we analyse spectral changes evident from the class means (Figure 1C) in more detail.

Univariate analysis of class means, revealed a very strong Raman peak at 782 cm^{-1} after 3 days of osteogenic COBs culture After 5 days of osteogenic culture, peak intensity decreases, suggesting a drop in DNA concentration. This peak increases between day 7 and day 14. The peak intensities extracted after deconvolution confirms this apparent change in DNA concentration (Figure 4A). In non- osteogenic COBs cultures, deconvolution of peak height intensities revealed that after the initial decrease between day 3 and day 5, very little change is detected between day 5 and day 7, but a considerable increase is shown between day 7 and 14 for the nucleic acid peak at 782 cm^{-1} (Figure S2D). Previous studies have indicated that DNA concentration in cells is related to proliferative status [45, 46]. Our data suggests that COBs are proliferating at first until confluence is reached (at day 5) at which point DNA concentration drops as the cells begin to differentiate. This is in keeping with current understanding of osteoblast behaviour in culture. After isolation, primary osteoblasts will first form collagen matrix and then proliferate on a surface; once confluence is reached, after around 7 days in culture, the fibroblast like pre-osteoblasts start to differentiate into a more mature form of osteoblast [47]. The Picogreen assay showed an increase in DNA concentration until day 7, which coincides with the switch from proliferation to differentiation at day 14 and a decrease in DNA concentration. Osteoblasts reach maturity after 14 days in culture [43]. Analysis of the Raman peaks indicates that after an initial drop in DNA at day 3, there is a gradual increase in proliferation up to day 14. This increase in DNA at day 14 coincides with an increase in extracellular matrix (ECM) associated Raman frequencies (Fig 4B) as well as ALP activity (Fig 2AB

399 and an overall increase in phosphate species present (supplementary
400 information Fig. S1). This behaviour suggests the COBs are differentiating and
401 preparing to start mineralising. Mature osteoblasts start to mineralise between
402 21 and 28 days and before that the extracellular matrix (ECM) comprising of
403 mainly collagen is laid down. By targeting the nuclei of individual cells, Raman
404 spectra retain the heterogeneous nature of primary osteoblasts in culture. To
405 isolate DNA from cells, it is necessary to lyse a large number of cells, thereby
406 losing the individual heterogeneity and any subtle variation that might be
407 present in population level concentrations.

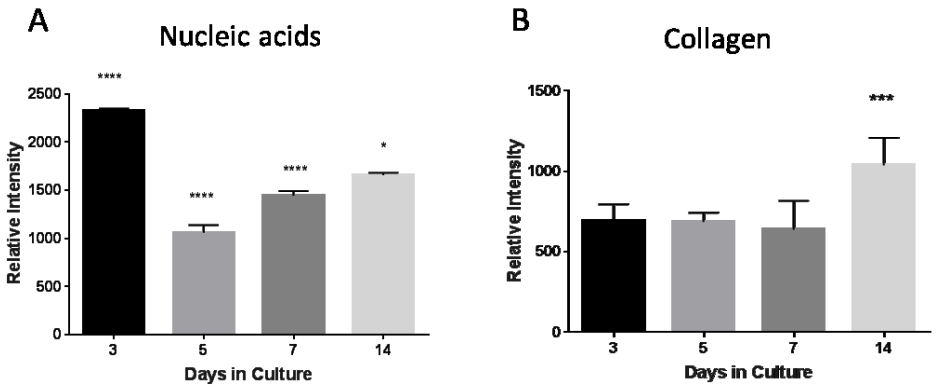

Figure 4. Raman spectral data analysis over time for COBs. Peak intensities for (A) Nnucleic acids (782 cm^{-1}) show gradual increase after day 5 of culture and (B) Collagen (CH_2 wag 1450 cm^{-1}) showing little change in peak height until day 14 of culture. Spectral deconvolution was carried out on averaged pre-processed spectra of COBs cultured each of the time points. Data is presented as the mean of deconvoluted peak intensity ± SEM ($p< 0.05$ *** $p<0.0001$ ****)

408 After 3 days of either osteogenic or non- osteogenic culture, ECM components
409 were detected using Raman spectroscopy. These have been previously
410 described and include bands at 852 cm^{-1} (C-C proline, hydroxyproline), 1003
411 cm^{-1} (phenyalanine ring breathing), 1255 cm^{-1} (Amide III), 1450 cm^{-1} (CH_2 wag)
412 and 1660 cm^{-1} (Amide I) [41, 48, 49].
413 The CH_2 wag, considered to be a component of collagen, was chosen for further
414 analysis of general matrix production [50-54]. Deconvolution analysis of peak
415 height was carried out on spectra from COBs cultured in osteogenic media.
416 There was no significant change in peak position or intensity in this component
417 of the collagen matrix over the early time points (Figure 4B). There is a
418 significant increase at day 14, which corresponds with increases in phosphate,
419 DNA and ALP activity. This compares well with the results from Sirius Red
420 staining where very little difference was detected in non-osteogenic COBs

cultures using the Sirius red collagen stain where an increased collagen staining was observed in the osteogenic cultures at day 14, but little difference visible in the early time points. This is similar to that observed with Raman spectroscopy (Figure 4B). The results with the controls (non-osteogenic cultures) are also largely similar in that there is a small increase at Day 14 and at other days over the time course there are little changes. Deconvolution of spectra taken of COBs grown in non- osteogenic medium also shows little change in the CH_2 wag matrix component before day 14 (Figure S2C). Until day 14 the ECM is dominated by a stable collagen component, the presence of the phosphate intermediates indicates that mineralisation has not yet taken place and the matrix is immature.

3.4 Raman spectroscopic analysis of phosphates in COBs

Osteoblasts ultimately form fully mineralised and mature bone which is primarily calcium hydroxyphosphate (hydroxyapatite or HA). However, before the stable form of hydroxyapatite is reached, a range of calcium phosphate intermediates can be formed. Amorphous calcium phosphate (ACP) is thought to be the first insoluble phase of calcium phosphate [55] This further goes through several intermediate forms and transient mineral species, including carbonated apatite (CAP) and octacalcium phosphate (OCP) before formation of hydroxyapatite (Figure 5). The presence of transient mineral species has previously been investigated in calvarial cultures and in the formation of bone in vivo [42, 48, 49].

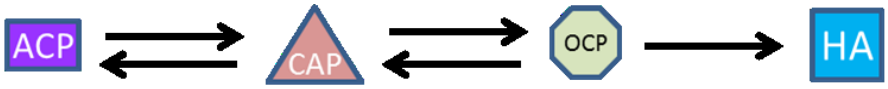

Figure 5. Reaction scheme representing the conversion of amorphous calcium phosphate (ACP) to crystalline hydroxyapatite (HA). Carbonated apatite (CAP) and octacalcium phosphate (OCP) are postulated as intermediate phosphates. The bi- directional arrows illustrate the transient nature of these phosphate intermediates.

In this study, particular attention was paid to the presence of intermediate calcium phosphate species; amorphous calcium phosphate (ACP 945-952 cm^{-1}) [42, 49], carbonated apatite (CAP 957-962 cm^{-1}) [41, 49] and octacalcium phosphate (OCP 970 cm^{-1}) [53, 56] (Table 1).

Table 1. Band assignments for Raman spectra of mineral components.

Raman Shifts (cm^{-1})	Band assignments	Component
945- 952	PO_4, P-O	ACP
955	not detected	OCP
957- 962	ν_1 PO_4, P-O	CAP
970	ν_1 PO_4, P-O	OCP

To track the transformation of phosphates from amorphous broad peaks to phosphates with more crystalline properties, deconvolution of peaks was carried out in the the $\nu_1 PO_4^{3-}$ spectral region between 948 and 970 cm^{-1} (zoomed in phosphate region is shown in Figure S3). While these peaks are not very pronounced their signal-to-noise ratio was >3 and therefore deconvolution was possible, as others have also previously shown [57]. Principal component analysis (PCA) on the phosphate spectral region was also carried out (Figure S3B). It establishes that while there is overlap between different time-points signifying similarity in spectral features there is some segregation (in PC1, PC3 and PC4) as well indicating differences between them despite lesser variables (due to the reduced spectral region analysed) in the PCA. Since the differences seem prominent enough in the class means we analysed the differences through deconvolution as described below.

In osteogenic COBs cultures, deconvolution of peak heights of combined phosphates between 948 cm^{-1} and 970 cm^{-1} show a decrease in phosphate peak height after day 3 (SI Figure S2A). In non- osteogenic COBs cultures, deconvolution of peak heights of combined phosphates show no change between day 3 and day 5. There is a decrease in peak height at day 7, followed by an increase at day 14 (SI figure S2B). More detailed analysis of osteogenic cultures of COBs, revealed that ACP is present with CAP at day 3 compared to other days while OCP is absent. Octacalcium phosphate (OCP) is a well-documented transient precursor to hydroxyapatite [42, 48, 49, 55]. OCP was detected only after 5 days of osteogenic COBs culture, together with a reduction in ACP and CAP (Figure 6A-C).

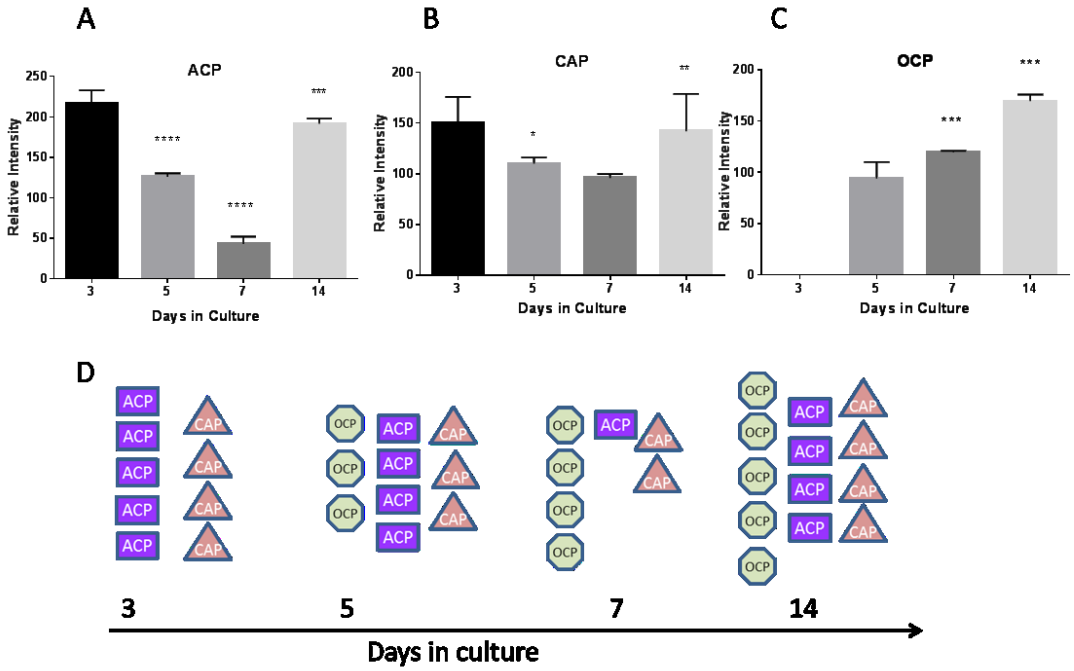

Figure 6. Modifications in phosphate species are evident from 5 days of calvarial osteoblast culture. Deconvolution analysis of phosphate species detected by Raman spectroscopy in COBs reveals alterations in amorphous calcium phosphate (A; ACP), carbonated apatite (B; CAP) and octacalcium phosphate (C; OCP). Data presented as mean of deconvolution ± SEM ($p < 0.05$ *** $p<0.0001$ ****). (D) Schematic representation of fluctuating concentrations of intermediate calcium phosphate species.

At day 7 of culture there is a significant decrease in ACP, a slight drop in CAP and increased OCP. After 14 days there is a dramatic increase in the presence of all phosphate species. This increase corresponds with a significant increase in ALP activity (Figure 2A), as well as increased collagen deposition (Figure 2B). Primary cells are heterogeneous in nature, they are known to contain cell populations at varying degrees of differentiation and maturity [58, 59]. This heterogeneity is evident in Raman spectra obtained from early time points (from day 3 to 5) which show a greater variability owing to differing levels of cell maturity. This could explain the presence of multiple phosphate species in COBs cultures. COBs are at different stages of differentiation and maturation and therefore differing phosphate species are present simultaneously. It has been suggested that the presence of pre-cursor phosphate species aids in the formation of hydroxyapatite, which could be considered the terminal product of mineral formation and the most stable calcium phosphate salt [60]. Early work by Brown *et al* reported on the existence of octacalcium phosphate (OCP) as a possible intermediate for hydroxyapatite and later went on to characterise the

Raman band assignment for OCP [56, 61]. Sometimes referred to as β- TCP, OCP is thought to have band positions located at 955 cm^{-1} and 970 cm^{-1}. In their study of calvarial cultures, Crane et al, report on the presence of an OCP like mineral at 955 cm^{-1}, but this mineral is not present in our COBs cultures [42]. An important pitfall was highlighted in a study by Stewart *et al*, where they describe the presence of β-TCP (975 cm^{-1}) in their MC3T3-E1 cell cultures as a consequence of the use of excess β- glycerophosphate [48]. It should be noted that the use of excess β- glycerophosphate (>5 mM) in osteoblast culture can lead to dystrophic mineralisation and impaired cell viability, this could also account for the presence of unexpected phosphate species [23, 62].

Multivariate analysis of COBs' spectra

Multivariate analysis was conducted by means of a pairwise comparison between each time point. Figure 7 represents the 3D scatterplots from the pairwise comparisons. Figure 7A shows the 3D plot of results attained from the PCA of Raman spectra collected from COBs cultured for 5 and 3 days. PC1, PC2 and PC3 represent 64.7%, 24.4% and 3.52% of the variance between the dataset respectively. With exception of one outlier, there is a distinct separation between day 5 and day 3. The PC1 loading (SI figure 4Ai) indicates that the entire spectrum contributes to the group separation between these time points. From the PC2 loading (SI figure 4Aii) Amide I, CH_2 wag and the 782 cm^{-1} peak appear to contribute most to the variance.

The 3D scatterplot for results obtained from the PCA of Raman spectra collected from day 7 and day 5 of culture, shows that although the time points remain clearly separated, the loadings are weighted differently this time. PC1 accounts for 71.3% of the variance, PC2 for 21.3% and PC3 for just 1.89% of the variance. The PC1 loadings (SI figure 4B i) are very similar to the PC1 loadings from day 5 and day 3, however, peaks in the phosphate symmetric stretch region (~950 cm^{-1}), though a small percentage, also contribute to the

variance in PC1. In PC2 the contribution of peaks in the phosphate symmetric stretch region contribute to a larger percentage of the overall variance.

The PCA analysis of Raman spectra collected from day 7 and day 14, as revealed by the 3D scatterplot shows the least amount of separation between the groups (Figure 7C). PC1 accounted for 50.5% of variance, PC2 43% and

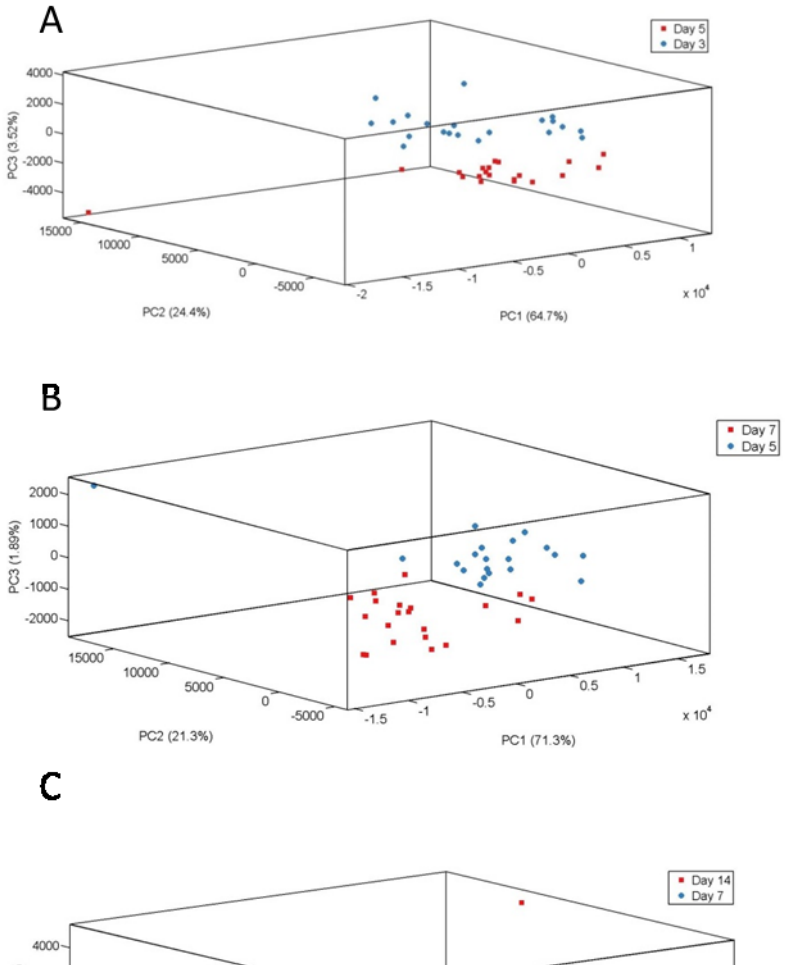

Figure 7. 3D scatterplots of pairwise PCA analysis output. (A) PCA analysis of day 5 and day 3 spectra of COBs. PC1, PC2 and PC3 represent 64.7%, 24.4% and 3.52% of the variance between the data set respectively. (B) PCA analysis of day 7 and day 5 spectra of COBs. PC1, PC2 and PC3 represent 71.3%, 21.3% and 1.89% of the variance between the data set respectively. (C) PCA analysis of day 14 and day 7 COBs. PC1, PC2 and PC3 represent 50.5%, 43% and 1.96% of the variance between the data set respectively.

PC3 1.96%. The components of PC1 are distinguishable as groups, but the components of PC2 are less obvious. It is noteworthy that the results from the ALP assay showed significant increases between cells cultured for 7 and 14 days in osteogenic media. The deconvolution analysis of the nucleic acid peak and the 1450 cm^{-1} collagen matrix peak also revealed significant differences between day 7 and 14. The PC1 loading (SI Figure 4Ci) of the PCA output of

the pairwise comparison between day 7 and 14 indicates that Amide I, CH_2 wag and Amide III contribute to the overall variance. The broad Amide III shoulder is dominated by matrix components. The Amide III shoulder visible in the class mean spectrum of COBs cultured for 14 days in osteogenic media (Figure 1C), appears to be more pronounced at day 14 when compared with day 7, suggesting changes in protein structure over time.

In general the PCA analysis has confirmed that there are significant differences between COBs cultured over time. Changes in matrix composition and structure contribute to these differences. Changes in the phosphate symmetric stretch were also detected, and appear to contribute to variance, though to a much lesser degree. In most cases the PC loadings indicate a lot of variation over the entire spectrum, and as such the subtle differences are lost. Deconvolution of individual peaks remains most appropriate to detect these subtle changes. The presence of OCP in Raman spectra, could be used as an early marker of osteogenic commitment, detectable before the onset of mineralisation and the appearance of HA. The ability of Raman spectroscopy to detect the presence of OCP before changes are apparent in ALP assay highlights the suitability of this technique to be used as a tool for characterising early cell behaviour.

4 Conclusion

Our results highlight the ability of Raman spectroscopy to detect subtle changes in osteoblast behaviour in primary cultures shortly after extraction from mice. Where the ALP assay was able to provide some information regarding changes in COBs' activity, by employing Raman spectroscopy, we could characterise a signature of early osteoblast behaviour by quantifying changes in DNA, phosphate species and collagen matrix during different stages of osteogenic commitment. Raman spectroscopy could indicate early changes and provide enhanced information regarding the phenotype of specific osteoblast populations which was not possible using conventional approaches. Whilst Raman spectroscopy could provide a means to assess the direct effects of growing cells on artificial implant substrates, we are not suggesting that the results of this study on quartz are applicable to all implant surfaces. This would,

however, only be possible if the Raman signals from the implant coatings could be differentiated from the signals generated by the cells or from boney outgrowths prior to osseointegration. Most importantly, if this caveat is taken into account, Raman spectroscopy has shown potential to be used to investigate early markers of differentiation in cells growing on implant coatings. It could be used as a predictor of potential bone outgrowth and osseointegration of these implants *in vivo*, which could lead to improved outcome of artificial implants.

Acknowledgements

Funding by Mathys Orthopedics (Switzerland) and University of Southampton Biological Sciences is kindly acknowledged. We also acknowledge the help provided by Justyna Smus.

References

1. Lavigne, P., et al., *Involvement of ICAM-1 in bone metabolism: a potential target in the treatment of bone diseases?* Expert Opinion on Biological Therapy, 2005. **5**(3): p. 313-320.

2. Simon, D.W.N., et al., *Identifying the cellular basis for reimplantation failure in repair of the rotator cuff.* Journal of Bone & Joint Surgery, British Volume, 2008. **90-B**(5): p. 680-684.

3. Wade-Gueye, N.M., et al., *Mice lacking bone sialoprotein (BSP) lose bone after ovariectomy and display skeletal site-specific response to intermittent PTH treatment.* Endocrinology, 2010. **151**(11): p. 5103-5113.

4. Shah, M., et al., *Local origins impart conserved bone type-related differences in human osteoblast behaviour.* European cells & materials, 2015. **29**: p. 155-176.

5. Zhang, B.G., et al., *Bioactive coatings for orthopaedic implants-recent trends in development of implant coatings.* International Journal of Molecular Sciences, 2014. **15**(7): p. 11878-921.

6. Nebe, J., et al., *Interface interactions of osteoblasts with structured titanium and the correlation between physicochemical characteristics and cell biological parameters.* Macromolecular bioscience, 2007. **7**(5): p. 567-578.

7. Olivares-Navarrete, R., et al., *Osteoblast maturation and new bone formation in response to titanium implant surface features are reduced with age.* Journal of Bone and Mineral Research, 2012. **27**(8): p. 1773-83.

8. Long, F., *Building strong bones: molecular regulation of the osteoblast lineage.* Nature Reviews Molecular Cell Biology, 2012. **13**(1): p. 27-38.

9. Komori, T., et al., *Targeted Disruption of Cbfa1 Results in a Complete Lack of Bone Formation owing to Maturational Arrest of Osteoblasts.* Cell, 1997. **89**(5): p. 755-764.

10. Ducy, P., et al., *Osf2/Cbfa1: A Transcriptional Activator of Osteoblast Differentiation.* Cell, 1997. **89**(5): p. 747-754.

11. Komori, T., *Regulation of osteoblast differentiation by transcription factors.* Journal of cellular biochemistry, 2006. **99**(5): p. 1233-1239.

12. Tonna, S. and N.A. Sims, *Talking among ourselves: paracrine control of bone formation within the osteoblast lineage.* Calcified Tissue International, 2014. **94**(1): p. 35-45.

13. Maes, C., et al., *Osteoblast precursors, but not mature osteoblasts, move into developing and fractured bones along with invading blood vessels.* Developmental Cell, 2010. **19**(2): p. 329-44.

14. Dirckx, N., M. Van Hul, and C. Maes, *Osteoblast recruitment to sites of bone formation in skeletal development, homeostasis, and regeneration.* Birth defects research. Part C, Embryo today : reviews 2013. **99**(3): p. 170-91.

15. Roberts, S., et al., *Functional Involvement of PHOSPHO1 in Matrix Vesicle–Mediated Skeletal Mineralization.* Journal of Bone and Mineral Research, 2007. **22**(4): p. 617-627.

16. Yadav, M.C., et al., *Loss of skeletal mineralization by the simultaneous ablation of PHOSPHO1 and alkaline phosphatase function: a unified model of the mechanisms of initiation of skeletal calcification.* Journal of Bone and Mineral Research, 2011. **26**(2): p. 286-97.

17. Nahar, N.N., et al., *Matrix vesicles are carriers of bone morphogenetic proteins (BMPs), vascular endothelial growth factor (VEGF), and noncollagenous matrix proteins.* Journal of Bone and Mineral Metabolism, 2008. **26**(5): p. 514-9.

18. Anderson, H.C., *Vesicles associated with calcification in the matrix of epiphyseal cartilage. .* The Journal of Cell Biology, 1969. **41**(1): p. 59-72.

19. Millan, J.L., *The role of phosphatases in the initiation of skeletal mineralization.* Calcified Tissue International, 2013. **93**(4): p. 299-306.

20. Golub, E.E., *Biomineralization and matrix vesicles in biology and pathology.* Seminars in Immunopathology, 2011. **33**(5): p. 409-417.

21. Stewart, A.J., et al., *The presence of PHOSPHO1 in matrix vesicles and its developmental expression prior to skeletal mineralization.* Bone, 2006. **39**(5): p. 1000-1007.

22. Taylor, S.E., M. Shah, and I.R. Orriss, *Generation of rodent and human osteoblasts.* Bonekey Reports, 2014. **3**: p. 585.

23. Orriss, I.R., et al., *Optimisation of the differing conditions required for bone formation in vitro by primary osteoblasts from mice and rats.* International journal of molecular medicine 2014. **34**(5): p. 1201-8.

24. Brauchle, E. and K. Schenke-Layland, *Raman spectroscopy in biomedicine – non-invasive in vitro analysis of cells and extracellular matrix components in tissues.* Biotechnology Journal, 2013. **8**(3): p. 288-297.

25. Buckley, K., et al., *Measurement of abnormal bone composition in vivo using noninvasive Raman spectroscopy.* IBMS BoneKEy, 2014. **11**.

26. Buckley, K., et al., *Towards the in vivo prediction of fragility fractures with Raman spectroscopy.* Journal of Raman Spectroscopy, 2015. **46**(7): p. 610-618.

27. McElderry, J.D., et al., *Tracking circadian rhythms of bone mineral deposition in murine calvarial organ cultures.* Journal of bone and mineral research 2013. **28**(8): p. 1846-54.

28. Ghita, A., et al., *Monitoring the mineralisation of bone nodules in vitro by space- and time-resolved Raman micro-spectroscopy.* Analyst, 2014. **139**(1): p. 55-8.

29. Gentleman, E., et al., *Comparative materials differences revealed in engineered bone as a function of cell-specific differentiation.* Nat Mater, 2009. **8**(9): p. 763-70.

30. Chiang, Y.-H., et al., *Raman spectroscopy for grading of live osteosarcoma cells.* Stem Cell Research & Therapy, 2015. **6**(1): p. 1-8.

31. McManus, L.L., et al., *Raman spectroscopic monitoring of the osteogenic differentiation of human mesenchymal stem cells.* Analyst, 2011. **136**(12): p. 2471-81.

32. Hung, P.-S., et al., *Detection of osteogenic differentiation by differential mineralized matrix production in mesenchymal stromal cells by Raman spectroscopy.* PloS one, 2013. **8**(5): p. e65438.

33. Trevisan, J., et al., *IRootLab: a free and open-source MATLAB toolbox for vibrational biospectroscopy data analysis.* Bioinformatics, 2013. **29**(8): p. 1095-1097.

34. Martin, F.L., et al., *Distinguishing cell types or populations based on the computational analysis of their infrared spectra.* Nature Protocols, 2010. **5**(11): p. 1748-1760.

35. Awonusi, A., M.D. Morris, and M.M.J. Tecklenburg, *Carbonate Assignment and Calibration in the Raman Spectrum of Apatite.* Calcified Tissue International, 2007. **81**(1): p. 46-52.

36. Puppels, G.J., et al., *Studying single living cells and chromosomes by confocal Raman microspectroscopy.* Nature, 1990. **347**(6290): p. 301-303.

37. Draux, F., et al., *Raman imaging of single living cells: probing effects of non-cytotoxic doses of an anti-cancer drug.* Analyst, 2011. **136**(13): p. 2718-2725.

38. Draux, F., et al., *Raman spectral imaging of single living cancer cells: a preliminary study.* Analyst, 2009. **134**(3): p. 542-548.

39. Meade, A.D., et al., *Growth substrate induced functional changes elucidated by FTIR and Raman spectroscopy in in–vitro cultured human keratinocytes.* Analytical and Bioanalytical Chemistry, 2007. **387**(5): p. 1717-1728.

40. Carden, A., *Application of Vibrational Spectroscopy to the study of calcified tissues.* Journal of Biomedical Optics, 2000. **5**(3): p. 259-268.

41. Mandair, G.S. and M.D. Morris, *Contributions of Raman spectroscopy to the understanding of bone strength.* BoneKEy Reports, 2015. **4**: p. 620.

42. Crane, N.J., et al., *Raman spectroscopic evidence for octacalcium phosphate and other transient mineral species deposited during intramembranous mineralization.* Bone, 2006. **39**(3): p. 434-442.

43. Hoemann, C.D., H. El-Gabalawy, and M.D. McKee, *In vitro osteogenesis assays: influence of the primary cell source on alkaline phosphatase activity and mineralization.* Pathologie Biologie (Paris), 2009. **57**(4): p. 318-23.

44. Weiss, M., et al., *Analysis of liver/bone/kidney alkaline phosphatase mRNA, DNA, and enzymatic activity in cultured skin fibroblasts from 14 unrelated patients with severe hypophosphatasia.* American journal of human genetics, 1989. **44**(5): p. 686.

45. Short, K.W., et al., *Raman Spectroscopy Detects Biochemical Changes Due to Proliferation in Mammalian Cell Cultures.* Biophysical Journal, 2005. **88**(6): p. 4274-4288.

46. Chan, J.W., et al., *Micro-Raman Spectroscopy Detects Individual Neoplastic and Normal Hematopoietic Cells.* Biophysical Journal, 2006. **90**(2): p. 648-656.

47. Cooper, L.F., *Biologic determinants of bone formation for osseointegration: Clues for future clinical improvements.* The Journal of Prosthetic Dentistry, 1998. **80**(4): p. 439-449.

48. Stewart, S., et al., *Trends in early mineralization of murine calvarial osteoblastic cultures: a Raman microscopic study.* Journal of Raman Spectroscopy, 2002. **33**(7): p. 536-543.

49. Tarnowski, C.P., M.A. Ignelzi, and M.D. Morris, *Mineralization of Developing Mouse Calvaria as Revealed by Raman Microspectroscopy.* Journal of Bone and Mineral Research, 2002. **17**(6): p. 1118-1126.

50. Rygula, A., et al., *Raman spectroscopy of proteins: a review.* Journal of Raman Spectroscopy, 2013. **44**(8): p. 1061-1076.

51. Wu, Y., et al., *Evaluation of the Bone-ligament and tendon insertions based on Raman spectrum and its PCA and CLS analysis.* Scientific Reports, 2017. **7**: p. 38706.

52. Salzer, R. and H.W. Siesler, *Infrared and Raman spectroscopic imaging*. 2009: John Wiley & Sons.

53. Inzana, J.A., et al., *Bone fragility beyond strength and mineral density: Raman spectroscopy predicts femoral fracture toughness in a murine model of rheumatoid arthritis.* Journal of Biomechanics, 2013. **46**(4): p. 723-30.

54. Shea, D.A. and M.D. Morris, *Bone Tissue Fluorescence Reduction for Visible Laser Raman Spectroscopy.* Applied Spectroscopy, 2002. **56**(2): p. 182-186.

55. Pompe, W., et al., *Octacalcium phosphate–a metastable mineral phase controls the evolution of scaffold forming proteins.* Journal of Materials Chemistry B, 2015. **3**(26): p. 5318-5329.

56. Brown, W.E., *Octacalcium Phosphate and Hydroxyapatite: Crystal Structure of Octacalcium Phosphate.* Nature, 1962. **196**(4859): p. 1048-1050.

57. Pezzotti, G., et al., *Raman spectroscopic investigation on the molecular structure of apatite and collagen in osteoporotic cortical bone.* Journal of the Mechanical Behavior of Biomedical Materials, 2017. **65**: p. 264-273.

58. Candeliere, G., F. Liu, and J. Aubin, *Individual osteoblasts in the developing calvaria express different gene repertoires.* Bone, 2001. **28**(4): p. 351-361.

59. Bianco, P., et al., *Bone sialoprotein (BSP) secretion and osteoblast differentiation: relationship to bromodeoxyuridine incorporation, alkaline*

phosphatase, and matrix deposition. Journal of Histochemistry & Cytochemistry, 1993. **41**(2): p. 183-191.

60. Koutsopoulos, S., *Synthesis and characterization of hydroxyapatite crystals: a review study on the analytical methods.* Journal of biomedical materials research, 2002. **62**(4): p. 600-612.

61. Fowler, B.O., M. Markovic, and W.E. Brown, *Octacalcium phosphate. 3. Infrared and Raman vibrational spectra.* Chemistry of Materials, 1993. **5**(10): p. 1417-1423.

62. Orriss, I.R., S.E.B. Taylor, and T.R. Arnett, *Rat Osteoblast Cultures*, in *Bone Research Protocols*, H.M. Helfrich and H.S. Ralston, Editors. 2012, Humana Press: Totowa, NJ. p. 31-41.